

Control of the propagation of intense laser pulses in gas for laser plasma acceleration

Danilo Giulietti,
Carlo A. Cecchetti,
Nadejda V. Drenska,
Riccardo Faccini,
Claudio Gatti,
Giancarlo Gatti,
Antonio Giulietti,
Leonida Gizzi,
Luca Labate,
Tadzio Levato,
Silvia Martellotti,
Naveen Pathak,
Paolo Valente

Abstract. The role of the propagation mechanisms of intense and ultra-short laser pulses in gas is presented, as well as the first results of the laser plasma acceleration (LPA) tests at Frascati National Laboratories (INFN), in the frame of NTA-PLASMONX project.

Key words: intense laser pulses • ultra-short laser pulse • laser plasma • plasma acceleration

D. Giulietti✉, N. Pathak
Physics Department of the University and National Institute of Nuclear Physics (INFN), Pisa, Italy and Intense Laser Irradiation Laboratory (ILIL), Istituto Nazionale di Ottica, UOS Adriano Gozzini, CNR, Pisa, Italy,
Tel.: +39 050 2214 840, Fax: +39 050 2214 333,
E-mail: danilo.giulietti@df.unipi.it

C. A. Cecchetti, A. Giulietti, L. Gizzi, L. Labate
Intense Laser Irradiation Laboratory (ILIL), Istituto Nazionale di Ottica, UOS Adriano Gozzini, CNR, Pisa, Italy

N. V. Drenska, R. Faccini, S. Martellotti, P. Valente
Physics Department of the University “La Sapienza” and National Institute of Nuclear Physics (INFN), Roma, Italy

C. Gatti, G. Gatti
LNF, National Institute of Nuclear Physics (INFN), Frascati, Italy

T. Levato
LNF, National Institute of Nuclear Physics (INFN), Frascati, Italy
and Intense Laser Irradiation Laboratory (ILIL), Istituto Nazionale di Ottica, UOS Adriano Gozzini, CNR, Pisa, Italy

Received: 1 October 2011

Accepted: 29 December 2011

Introduction

The advent of the chirped pulse amplification (CPA) [14] technique has made experimentally accessible the laser plasma acceleration (LPA) originally proposed in the late 1970s [15]. In fact the excitation of the plasma wave is strongly enhanced when the length of an intense laser pulse fits in half of the plasma wavelength $\lambda_p \approx 2\pi c/\omega_p$, $\omega_p = \sqrt{4\pi n_e e^2/m_e}$ being the so-called plasma frequency. In this case the ponderomotive force associated with the laser pulse expels electrons from a region whose dimension matches the one of a density minimum region of a plasma wave. With this respect, this wake-field generation process can be considered as quasi-resonant. For ultra-short laser pulses such a condition is fulfilled at relatively high plasma densities n_e , at which the accelerating electric fields of plasma waves can be extremely high, being proportional to $\varepsilon\sqrt{n_e}$, where $\varepsilon = (\Delta n_e/n_e)$ is the amplitude of the electron density perturbation.

The experimental and theoretical activity in LPA has been in the last years exceptionally intense and very rich of impressive results. In the next future we expect even more relevant results, as those pursued by the BELLA project, under realization at LBNL by the Wim Leemans group [9]. Also Italy is intensifying the engagement in this field. In fact the National Institute of Nuclear Physics (INFN) has recently launched the Strategic Project NTA-PLASMONX [6] in which LPA techniques will be exploited using a 250TW Ti:Sa laser, synchronized with an advanced 150 MeV LINAC.

Generation of laser pulses with duration of tens of femtosecond necessarily implies that several effects oc-

curing in the complex laser chain can affect the final delivered pulse. One of the most relevant problems is the presence of precursors in the temporal profile of the laser pulse. There are at least three main sources of such precursors: oscillator background, amplified spontaneous emission (ASE) and imperfect compression of the stretched amplified pulse in the CPA system. Depending on the ratio of the power of such precursors with respect to the peak power of the main short pulse (normally between 10^6 and 10^{10}), and considering that this latter is usually focused at intensities that easily exceed $I = 10^{19} \text{ W}\cdot\text{cm}^{-2}$, the intensity of the precursors can be well above the ionization threshold of the majority of targets (either solids or gases). This occurrence changes radically the scenario of the laser interaction with the target, since it can happen that the short femtosecond pulse interacts with a pre-plasma rather than the solid or gaseous medium. Obviously the interaction conditions also depend on the timing and duration of the precursor with respect to the main pulse, as the preformed plasma evolves prior to the high-intensity interaction. In fact, even in the cases in which the pre-pulse action can be ignored, the ionization of the medium by the main pulse can deeply change its propagation due to self phase modulation and self defocusing caused by the fast change in the refractive index or generation of intense local electric and magnetic fields.

Because the plasma produced by the precursor pulse has the time to hydrodynamically evolve, its evolution can be used to make the plasma as suitable as possible for an improved propagation of the main pulse and consequent efficient acceleration.

Propagation of ultra-short super-intense laser pulses in gas

A pioneering experiment on laser guiding was performed in the late 1980s [7]. Two collinear Q-switching Nd-laser pulses, separated each other of few nanoseconds, were focused on an under-dense plasma. While the first pulse was strongly diffracted as a consequence of the suffered self-focusing effects, the second one propagated almost un-attenuated for several Rayleigh lengths in a low density channel formed by the first one.

More recently, the same group conceived an experiment oriented to find the most suitable conditions to improve the acceleration length in LPA technique, producing hollow cylindrical plasmas for guiding intense laser pulses [4]. To do so, an experimental arrangement to probe the laser-gas-jet interaction with a fast interferometric technique was setup at the Intense Laser Irradiation Laboratory (ILIL) of INO-CNR in Pisa (Italy). The laser system employed to study the plasma evolution driven by an ASE-like laser pulse is a 3.3 GW Nd:YLF delivering two beams with a maximum energy of 5 J per beam at a wavelength of 1053 nm and duration of 3 ns FWHM. The system can provide intensities up to $10^{15} \text{ W}\cdot\text{cm}^{-2}$ on a target with a high temporal and spatial quality. The laser works in single mode both longitudinally and transversely. One of the two beams (main) is used for the interaction with the target, while the other (probe) is used for interferometry. The probe beam is frequency doubled by a KDP-type crystal, so that λ_{probe}

= 527 nm and is filtered from any remained infra-red fraction of the pulse. In order to probe the evolution of the plasma at different delays with respect to its creation by the main pulse, the probe beam is sent on an optical delay-line. The probe beam crosses then the sample in orthogonal direction with respect to the main pulse propagation direction, and enters the interferometer setup, after which is imaged on a CCD camera. The interferometer is built in Nomarski configuration. The transmitted main pulse is also imaged on a CCD camera in order to monitor the equivalent focal plane, and to image the position of the laser focus with respect to the target. In this study, in fact, a careful control on the laser point of interaction with the gas is needed to systematically characterize the produced plasma. The main pulse is focused on the target with a $f/8$ lens, and the resulting focal spot is almost elliptical with semi-axis of dimension $(5.2 \pm 0.2) \mu\text{m}$ and $(6.0 \pm 0.2) \mu\text{m}$. This implies that the Rayleigh length in this case is $Z_R = (\pi w_0^2/\lambda) \approx 10 \mu\text{m}$. In order to have an intensity for the main pulse, that is of the order of $10^{13+14} \text{ W}\cdot\text{cm}^{-2}$, the energy of the laser pulses was set in the range 0.3 to 0.5 J by tuning the system's amplifiers. For what concerns the intensity of the main beam, it implies that, given the fraction of energy actually reaching the target of the order of 80%, the intensity on target is approximately $1.4 \times 10^{14} \text{ W}\cdot\text{cm}^{-2}$. In order to produce a high-density gas column (up to 10^{20} cm^{-3}), a subsonic gas-jet coupled with a stainless steel, high-speed solenoid valve was used for. The valve could operate at 10 Hz repetition rate with backing pressure up to 20 bar. The opening duration of the electro-valve was estimated to be 10 ms FWHM. The gas-jet density distribution coming from different nozzles coupled to this kind of electro-valve has been formerly characterized in detail with fast interferometric techniques. In the following description, we will present results obtained with a rectangular slit nozzle with dimension of 3 mm in length and 0.3 mm in width. Due to the subsonic nature of the gas-jet, the gas expands well beyond the size of the slit after its exit from the nozzle. A schematic view of the interaction is shown in Fig. 1. The gas used in the experiment is helium, whose backing pressure varied from 5 to 8 bar.

Among the huge number of collected interferograms, in the following the one relevant to the best interaction conditions for LPA is presented. From the experiment, it results that a small plasma is initially pro-

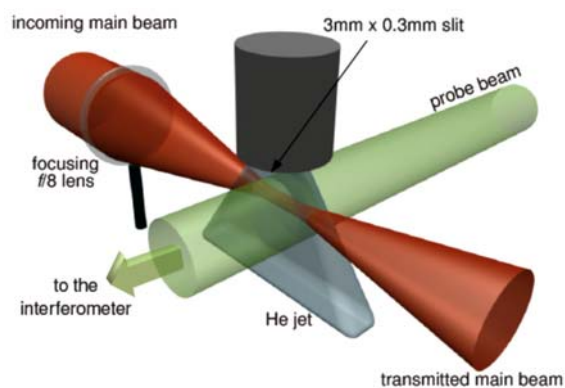


Fig. 1. Scheme of the interaction region with the propagating main and probe pulses.

duced by optical breakdown in the gas nearby the focus; then the plasma expands along the laser propagation axis. This expansion is due to the fastest of the following two phenomena: (i) the “propagation” of the condition for the optical breakdown at the leading edge of the laser pulse, or (ii) the propagation of the blast wave produced by the local fast heating of the gas. The most interesting condition leading to relevant data for laser wake-field acceleration (LWFA) was found focusing the main laser beam $500\ \mu\text{m}$ away from the nozzle slit plane. At this distance from the nozzle, the helium density in the jet is of the order of $5 \times 10^{18}\ \text{cm}^{-3}$. Deconvoluted data demonstrate the production of quasi-cylindrical plasmas extending over several millimeters and with a hollow density channel on their axis (see Fig. 2). The mean on-axis electron plasma density ranges from 3.5 to $4.5 \times 10^{18}\ \text{cm}^{-3}$. As a speculation, it can be noted that these values of electron density are quasi-resonant in the LWFA regime with laser pulses of duration $\tau \approx 30$ fs FWHM. The density along the longitudinal axis smoothly rises in the direction of the laser propagation up to a maximum density of roughly $10^{19}\ \text{cm}^{-3}$, located at the end of the channel, constituting a sort of “tip” with a few tens of μm ’s width. It is worth noting how the obtained plasmas present only a single-end tip, while on

the opposite side on the channel longitudinal axis the plasma has a rather smooth descending to-zero slope. This is due to the fact that, except for the case in which the laser is focused at the centre of the gas-jet, one edge of the plasma falls in a region of lower gas density (either the entrance or the exit) where boundaries of the jet are located. For what concerns the transverse density profile, the density minimum has a value in the range of 60 to 70% with respect to the channel walls, while its radius r_{ch} at half of the depth is of the order of 30 to 50 μm . These values are suitable to optically guide a driving pulse. The density distribution in Fig. 2d can be described as $n(r) = n_0 + \Delta n(r/r_{ch})^2$, given that the values for n_0 and $\Delta n/r_{ch}^2$ resulting from the fit are $4.54 \times 10^{18}\ \text{cm}^{-3}$ and $3.74 \times 10^{22}\ \text{cm}^{-5}$, respectively. With reference to equation $w_0 = (r_{ch}^2/\pi r_e \Delta n)^{1/4}$, which relates the plasma channel density profile with the laser spot size to match the optical guiding condition [4], the obtained data are consistent with $w_0 = 23\ \mu\text{m}$. It means that pulses focused in spots smaller than w_0 can be refractive-guided in such plasma channels.

Plasmas similar to that reported in Fig. 2 are found to be suitable for refractive laser-guiding over many Rayleigh ranges [2, 13], opening to an efficient use in high gain, long-scale acceleration experiments.

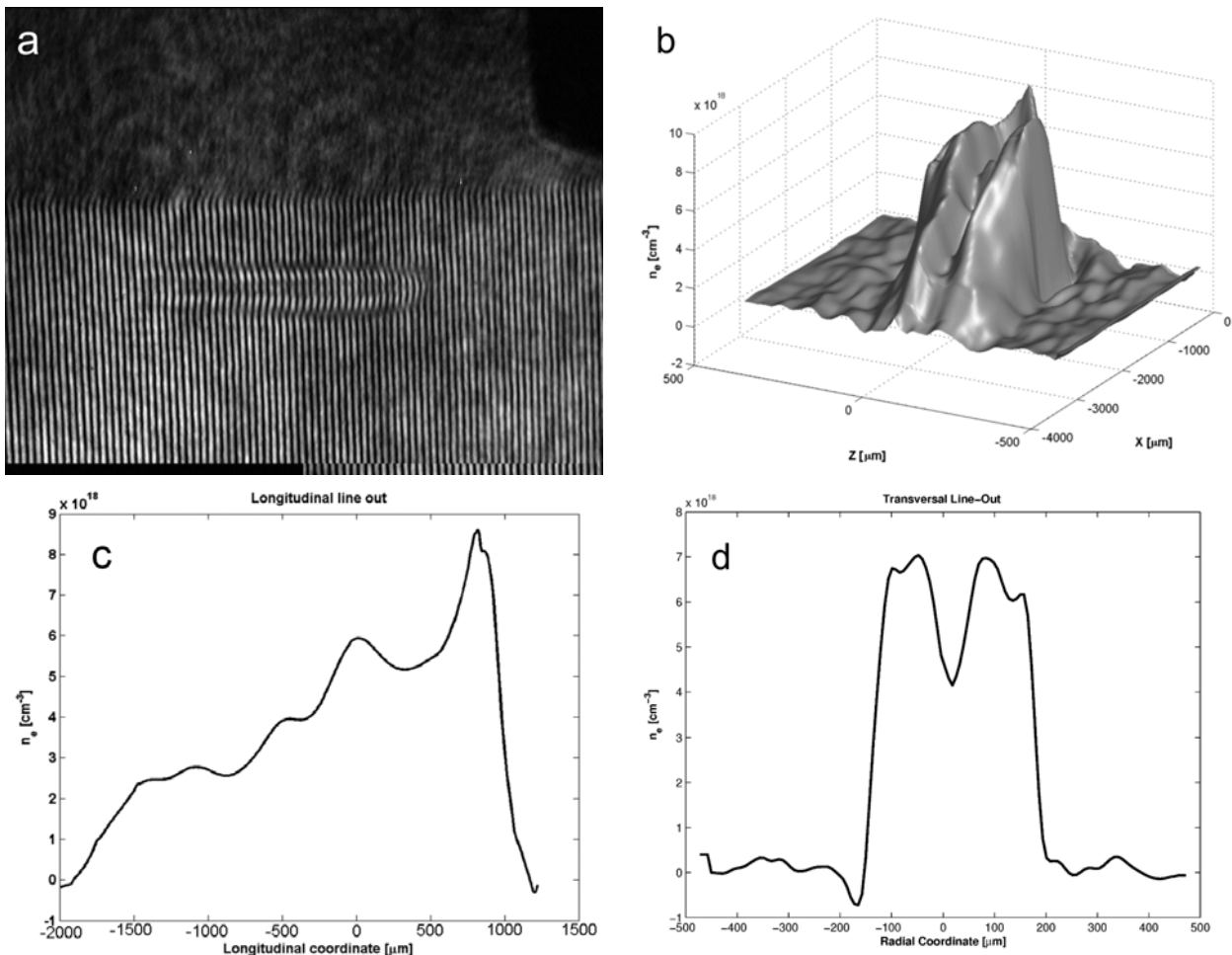


Fig. 2. (a) Interferogram of the interaction region when 460 mJ, 3 ns FWHM neodymium laser pulse is focused at the entrance of helium gas-jet, $500\ \mu\text{m}$ away from the nozzle slit plane. At this distance from the nozzle, the neutral helium density is about $5 \times 10^{18}\ \text{cm}^{-3}$. The laser pulse propagates from the left side of the image. (b) 3-D electron density map obtained after the analysis of interferogram reported in (a). (c) Density lineout taken on the longitudinal axis. (d) Density lineout taken at $300\ \mu\text{m}$ from the entrance of the gas-jet in the transverse direction.

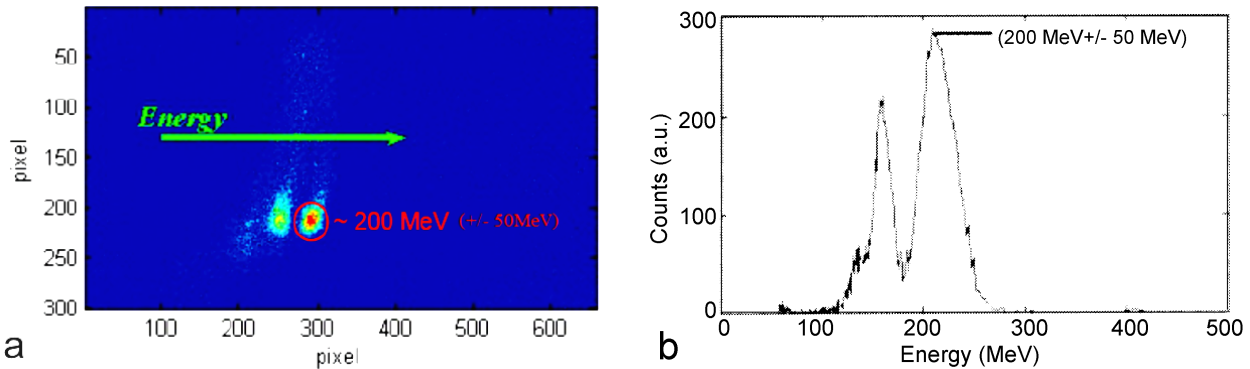


Fig. 3. Electron bunch detected on LANEX after deflection in the magnetic spectrometer (a) and corresponding horizontal lineout (b). The uncertainty in the energy measurement is ± 50 MeV.

Laser plasma acceleration in LNF

The role played by the laser guiding in LPA has been evidenced also in a recent experiment performed in the PLASMONX [8] laboratory at LNF-INFN, where 30 TW, 30 fs pulses from a Ti:Sa laser were focused on a supersonic gas-jet at an intensity of $I \approx 6 \times 10^{18} \text{ W}\cdot\text{cm}^{-2}$. The plasma electron density of the ionized N_2 at $\approx 7\text{--}12$ bar backing pressure was $n_e \approx 10^{19} \text{ cm}^{-3}$. Figure 3a shows the image of the electron bunch detected by a LANEX screen after dispersion in the 0.9 T magnetic spectrometer, while Fig. 3b shows the corresponding lineout together with a calibrated energy scale. During the experiment, mainly devoted to individuate the best conditions for LPA, the magnetic spectrometer was operated without the usual entrance slit. So, while the vertical dimension of the electron bunch on the LANEX depends on its divergence (≈ 5 mrad), the horizontal one depends also on its energy spread. The two dimensions being more or less the same (spot almost circular) it evidences that the electron bunch energy spread is less than the one you can deduce from the LANEX image, i.e. $\Delta E/E < 10\%$. In the experiment the activated Thomson scattering (TS) diagnostic evidenced the extension of acceleration length (≈ 2 mm), more than 4 times the Rayleigh length of the employed focusing optics, due to the onset of the relativistic self-focusing, whose threshold power was, in our experimental conditions, $P_c = (2m^2c^5/e^2) \cdot (n_e/n_e) \approx 17(n_e/n_e) \text{ GW} \approx 3 \text{ TW}$. The Thomson scattering diagnostics together with the direct imaging of the electron bunch on LANEX screen also shows the formation of two acceleration “channels”, due to the splitting of the main laser beam, most probably a consequence of aberrations on the main laser beam.

Conclusions and perspectives

At present, several regimes for LPA have been successfully investigated, aimed to optimize the maximum energy, the energy spread, the charge and divergence of the accelerated bunches [1, 3, 5, 10–12]. The extension of the acceleration length, largely overcoming the Rayleigh length, is tempted following different experimental strategies; among them the control of the propagation of the intense laser pulse in the gases or plasmas confined in different ways (cells, capillaries,...). Most probably the next challenge will be the staged injection, in which in a first cell a bunch of energetic and

quite monochromatic electrons is created by ionization injection [1] and further accelerated in a second stage, setup to work in the external-injection regime.

Acknowledgment. The experimental results presented in this paper have been obtained in the frame of the collaboration with the colleagues of the Strategic INFN Project NTA-PLASMONX and the Istituto Nazionale di Ottica, Pisa (CNR).

References

1. Clayton CE, Ralph JE, Albert F *et al.* (2010) Self-guided laser wakefield acceleration beyond 1 GeV using ionization-induced injection. *Phys Rev Lett* 105:105003
2. Esarey E, Sprangle P, Krall J, Ting A (1997) Self-focusing and guiding of short laser pulses in ionizing gases and plasmas. *IEEE J Quantum Electr* 33:1879–1914
3. Faure J, Glinec Y, Pukhov A *et al.* (2004) A laser-plasma accelerator producing monoenergetic electron beams. *Nature* 431:541–544
4. Gamucci A, Galimberti M, Giulietti D *et al.* (2006) Production of hollow cylindrical plasmas for laser guiding in acceleration experiments. *Appl Phys B* 85:611–617
5. Geddes CGR, Toth Cs, van Tilborg J *et al.* (2004) High-quality electron beams from a laser wakefield accelerator using plasma-channel guiding. *Nature* 431:538–541
6. Giulietti D, Macchi A (2007) Super-intense LASERS for everybody. *Il Nuovo Saggiatore* 23:3–4 (<http://www.inf.infn.it/acceleratori/plasmonx/>)
7. Giulietti A, Vaselli M, Cornolti F, Giulietti D, Lucchesi M (1987) Laser beam self-focusing during the production of an underdense plasma with nanosecond pulses. *Rev Roum Phys* 32:23–27
8. Gizzi LA, Anelli F, Benedetti C *et al.* (2009) Laser-plasma acceleration with self-injection: A test experiment for the sub-PW FLAME laser system at LNF-Frascati. *Il Nuovo Cimento C* 32:433–436
9. <http://newscenter.lbl.gov/news-releases/2009/06/25/bella-accelerating-electrons/>
10. Leemans WP, Nagler B, Gonsalves AJ *et al.* (2006) GeV electron beams from a centimetre-scale accelerator. *Nat Phys* 2:696–699
11. Mangles SPD, Murphy CD, Najmudin Z *et al.* (2004) Monoenergetic beams of relativistic electrons from intense laser-plasma interactions. *Nature* 431:535–538
12. Pukhov A, Gordienko S, Kiselev S, Kostyukov I (2004) The bubble regime of laser-plasma acceleration: monoenergetic electrons and the scalability. *Plasma Phys Control Fusion* 46:B179–B186

13. Sprangle P, Esarey E, Ting A (1990) Nonlinear interaction of intense laser pulses in plasmas. *Phys Rev A* 41:4463–4469
14. Strickland D, Mourou G (1985) Compression of amplified chirped optical pulses. *Opt Commun* 56:219–221
15. Tajima T, Dawson J (1979) Laser electron accelerator. *Phys Rev Lett* 43:267–270